Applied Energy 358 (2024) 122619

Contents lists available at ScienceDirect

Applied Energy

journal homepage: www.elsevier.com/locate/apenergy

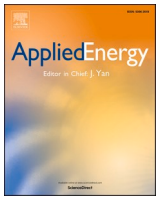

A data-driven framework for designing a renewable energy community based on the integration of machine learning model with life cycle assessment and life cycle cost parameters

Youssef Elomari [a], Carles Mateu [a,b], M. Marín-Genescà [a], Dieter Boer [a,*]

[a] Departament d'Enginyeria Mecànica, Universitat Rovira i Virgili, Av. Països Catalans 26, 43007 Tarragona, Spain
[b] Department of Computer Science and Industrial Engineering, University of Lleida, 25001 Lleida, Spain

HIGHLIGHTS

- A data-driven framework for optimizing the residential renewable energy community is framed.
- The framework is applied to a real case study residential community in Tarragona, Spain.
- Multi-objective optimization is applied to minimize LCC and LCA parameters while maximizing green energy use.
- A multi-criteria decision-making approach is carried out to design optimized configurations for energy communities.

GRAPHICAL ABSTRACT

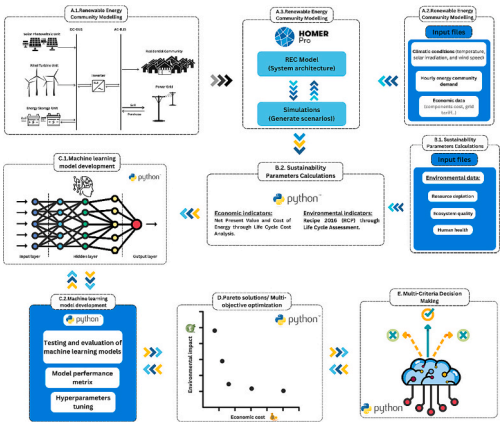

ARTICLE INFO

Keywords:
Energy community
Optimization
Machine learning
Life cycle assessment
Life cycle cost
Multi-objective optimization
Multi-criteria decision making

ABSTRACT

This research paper presents a data-driven framework for design optimization of renewable energy communities (RECs) in the residential sector, considering both techno-economic challenges and environmental impact. The study's focus is to determine suitable sizes for photovoltaic systems, wind turbines, and battery electrical energy systems by evaluating energy, economic, and environmental criteria. To achieve this, we develop a data-driven model that incorporates Homer Pro and an in-house tool developed in Python programming language that integrates a machine learning algorithm, life cycle cost (LCC), life cycle assessment (LCA) calculations of the REC model. Furthermore, a multi-objective optimization model is established to minimize the LCC and LCA parameters while maximizing green energy use. Moreover, a multi-criteria decision-making approach based on Weighted Sum Model (WSM) is proposed to help the stakeholders to see beyond the selection criteria based on LCC and LCA to choose the most appropriate scenario optimal solution for the desired energy community and interpret the effect of various economic parameters on the sustainable performance of REC. The framework

* Corresponding author.
E-mail addresses: youssef.elomari@urv.cat (Y. Elomari), carles.mateu@udl.cat (C. Mateu), marc.marin@urv.cat (M. Marín-Genescà), dieter.boer@urv.cat (D. Boer).

https://doi.org/10.1016/j.apenergy.2024.122619
Received 19 September 2023; Received in revised form 12 December 2023; Accepted 3 January 2024
Available online 12 January 2024

application is illustrated through a case study for the optimal design of REC for a residential community in Tarragona, Spain, consisting of 100 buildings. The results revealed a substantial improvement in economic and environmental benefits for designing REC, the optimal minimum cost solution with a levelized cost of energy (LCOE = 0.044 $/kWh) and a payback period of 7.1 years with an LCOE reduction of 85.04% compared to the base case. The minimum impact with an LCOE = 0.220 $/kWh and a payback period of 12.5 years with a reduction in environmental impact of 54.59% compared to the base case. Overall, the developed data-driven provides policy decision-making with an evaluation of REC in the residential sector.

Abbreviations

ANN	Artificial Neural Network
BEES	Battery Electrical Energy Storage
CC	Capital cost
CRF	Capital Recovery Factor
EVS	Explained Variance Score
HOMER	Hybrid Optimization Model for Electric Renewables
LCA	Life Cycle Assessment
LCC	Life Cycle Cost
LCIA	Life Cycle Impact Analysis
LCOE	Levelized Cost of Energy
MAE	Mean Absolute Error
ML	Machine Learning
MOO	Multi-Objective Optimization
NPC	Net Present Cost
O&M	Operation and Maintenance
PV	Photovoltaics
R2	R-squared
RC	Replacement cost
REC	Renewable Energy Community
RESs	Renewable Energy Sources
WT	Wind Turbine

Nomenclature

Ah	Ampere hours
$C_{ann,tot}$	Annualized cost ($/year)
CRF	capital recovery factor
DAM_d	indicator results for damage category d
DOD	battery system depth of discharge
$E_{prim,AC}$	AC primary load served (kWh/year)
$E_{prim,DC}$	DC primary load served (kWh/year)
$E_{grid,sales}$	total grid sales (kWh/year)
E_d	daily energy demand (kWh)
f_{PV}	PV array's derating factor (%)
G_T	incident solar radiation in the current time step (kW/m2)
$G_{T,STC}$	incident solar radiation at the standard temperature condition (kW/m2)
i	real interest rate (%)
LCI_i^{MP}	manufacturing processes associated with the elementary flow i
LCI_i^{OP}	plant operation associated with the elementary flow i
LCI_i^{TOT}	total life cycle inventory associated with the elementary flow i
LCI_i^{TR}	transportation tasks associated with the elementary flow i
n_d	days of autonomy
P_{WTG}	power generation of wind turbine (kW)
$P_{WTG,STC}$	wind turbine output at the standard condition (kW)
RCP	ReCiPe 2016 aggregated impact factor (Pts)
R_{proj}	project lifetime (year)
T_C	PV's temperature (°C)
$T_{C,NOCT}$	nominal operating PV cell temperature (°C)
$T_{C,STC}$	PV array's temperature at the standard temperature conditions (°C)
U_{anem}	wind speed at anemometer height (m/s)
U_{hub}	wind speed at the hub of the wind turbine (m/s)
V_{bat}	battery voltage (V)
Y_{PV}	PV output under typical operating conditions (kW)
z_{hub}	anemometer height above the surface (m)
z_0	anemometer height (m)

Greek symbols

α_P	temperature coefficient of power measured in (%/°C)
α	solar absorption
τ	solar transmittance of the PV array
η_c	electrical conversion efficiency of the PV array
$\eta_{mp,STC}$	the maximum power point efficiency under standard test conditions, expressed in (%)
ε_d	weight factor based on values recommended in the ReCiPe 2016 framework
δ_{dis}	factor is based on the use of land and extraction of materials in the European setting
Θ_{ei}	characterization factor that connects endpoint impact category e with the elementary flow i
ρ	actual air density
ρ_0	air density at standard condition

Indices

d	damage category
i	elementary flow
N	number of years

1. Introduction

Due to its potential for addressing problems caused by climate change and the demand for sustainable energy, incorporating renewable energy sources has attracted considerable attention in recent years [1]. Exploring alternative energy options can help to reduce greenhouse gas emissions [2]. The building sector consumes a large amount of energy and natural resources, with negative impact on the environment. For instance, 50% of energy usage, 33% of water use, 50% of raw material extraction, and 40% of greenhouse gas emissions in Europe are attributed to buildings [3,4]. The Sustainable Development Goals (SDGs) of the United Nations (UN) emphasize the necessity of addressing these effects and identify the construction industry as a critical participant in attaining environmental goals on a local and global scale [5].

Following this, the European Commission has established challenging goals to make sure that by 2030, renewable sources will constitute 45% of its energy mix [6]. This commitment entails a significant boost in the ability to generate renewable energy, particularly emphasizing the quick adoption of solar photovoltaics (PV). In order to fuel the expansion of renewable energy, it is planned to install more than 320 GW of PV by 2025 and approximately 600 GW by 2030 in the European Union [7].

Energy communities have become a viable strategy to enable the integration of renewable energy into the building industry [8]. An energy community is a gathering of energy producers and consumers who collaborate for the purpose of optimizing energy production, consumption, and distribution [9,10]. Local energy communities that pool resources and share energy encourage the use of renewable energy technology, enable energy independence, encourage sustainable behaviors, and decrease dependency on fossil fuels [11].

Several technical, economic, and environmental problems arise with the idea of an energy community. The integration of renewable energy resources requires the use of cutting-edge technology [11], such as smart grids [12], energy storage systems [13,14], and demand response mechanisms [12]. These technologies allow for effective energy management [15], grid stability [16], and optimum energy flows within the community [12]. Additionally, there are economic considerations since energy communities can result in cost reductions, income production via energy trading, and the development of jobs for the community's economy [17,18]. Furthermore, energy communities provide significant environmental advantages, such as lower carbon emissions, better air quality, and greater resilience to the consequences of climate change [19].

Renewable energy communities (RECs) are becoming more important worldwide. There are examples of practical applications, including those in Beijing [20], Wuhan [21], and Melbourne [22]. Additionally, since the EU RED II Directive was adopted in 2018 [23], RECs have become an important topic for European renewable energy systems. The design of the REC includes a number of elements, including the selection and size of renewable energy sources, energy storage systems, and the implementation of energy-efficient building design principles. The location and layout of the community, the local climate, the availability of renewable energy sources, the storage capacity, the demand profile, and the energy demand are all crucial elements in making the most use of the available resources.

To optimize an energy community, it is necessary to maximize the usage of RESs and achieve the best possible energy balance [24,25]. This requires the development along with the implementation of complex modeling techniques and optimization algorithms [38]. These optimization methods could assist a community in developing an energy mix that is both economically and environmentally sustainable, boosting energy independence and lowering dependency on the grid [26,27]. Several tools have been developed for this method of modeling, including the hybrid optimization model for electric renewables (HOMER) [28], the distributed energy resources-consumer adoption model (DER-CAM) [29], and REopt [30]. Tozzi et al. [31] conducted an extended comparison of the most used renewable energy simulation tools at the community level. Furthermore, the authors found that the accuracy of renewable energy simulation tools is enhanced through high-quality imported data containing relevant and specific information.

Several studies have been conducted to investigate and develop efficient approaches with the goal of enhancing size and cost control as well as increasing overall efficiency. These methodologies include a variety of strategies, such as genetic algorithms [32], hybrid genetic algorithms [33], iterative techniques [34,35], graded particle swarm optimizations [36], and Meta Particle Swarm Optimization [31,32,37].

The best energy mix scenario within a community that uses renewable energy sources could also be designed using machine learning techniques. These algorithms can evaluate and deal with complicated data sets, such as energy demand profile, weather predictions, and profiles of renewable energy generation [39]. in order to optimize energy generation, consumption, and distribution. It is feasible to develop prediction models using machine learning approaches that allow for the identification of the optimum combination of renewable energy technologies, storage systems, and energy management techniques [39]. There has been research employing machine learning, such as Ferrara et al. [40] developed a deep residual learning-based method to simplify the Nearly Zero Energy Building optimization design. Waqar et al. [41] proposed a machine learning algorithm-based energy management of the renewable energy community in the smart grid. Kumar et al. [42] employed artificial neural networks to predict the size, tilt, and azimuth angles of PV systems. Khatib and Elmenreich [43] employed a Generalized Regression Neural Network to predict the PV array and battery size ratio. Achieving the most effective and sustainable energy mix scenario could be achievable with the integration of machine learning algorithms, which could allow energy communities to make intelligent decisions.

The novelty of our research is the development a data-driven framework to design the renewable energy community (REC) considering its techno-economic failures and environmental impact. In order to assist the stakeholders' decision-making, the study tends to optimize the size of the REC source of energy technologies used (such as photovoltaic systems, wind turbines, and battery electrical energy systems) under energy, economic, and environmental criteria. In this context, Homer Pro and an in-house tool developed in Python programming that incorporates a machine learning algorithm, life cycle cost (LCC), life cycle approach (LCA) calculations of REC model. Furthermore, A multi-objective optimization model is established to minimize the LCC and LCA parameters with consideration for maximizing green energy use. Additionally, a multi-criteria decision-making approach based on Weighted Sum Model (WSM) is proposed to help the stakeholders to see beyond the LCC and LCA based on selection criteria to choose the most appropriate scenario optimal solution for the desired energy community and interpret the effect of various economic parameters on the sustainability of REC. The proposed methodology can serve as valuable insights and practical guidelines for policymakers, energy planners, and building professionals interested in promoting the integration of renewable energy within the building sector by establishing energy communities. The paper is structured as follows: Sections 2 and 3 illustrate the research methodology framework and the case study description of this study. Afterward, the optimization results and the findings of this study are reported and discussed in Section 4. The paper concludes by highlighting the main results in Section 5.

2. Methodology framework

The proposed methodology framework for the optimal design of the renewable energy community is outlined in Fig. 1. The framework consists of five primary phases: renewable energy community modeling (A) using Homer Pro software to design and generate scenarios, a Python in-house tool was used for; sustainability parameters calculations (B), and also for machine learning model development (C), Pareto solutions/multi-objective optimization (D) for economic and environmental objectives. and later multi-criteria decision-making (E) to facilitate the selection according to the needs/preferences of stakeholders.

2.1. Energy system description

A typology of a renewable energy community system is designed for a residential neighborhood of 100 buildings in Tarragona, Spain, to cover the energy demand, as shown in Fig. 2. The system architecture incorporates a solar photovoltaic unit, wind turbine unit, energy storage unit, inverter, the power source from the utility, and the residential community load. Homer Pro software has been used to model and simulate the renewable energy community system.

2.1.1. Mathematical model

a. Photovoltaic system

The photovoltaic system incorporates renewable energy into the system by supplying the DC-BUS with renewable electricity. The PV power generation can be calculated as stated in Eq. (1) below:

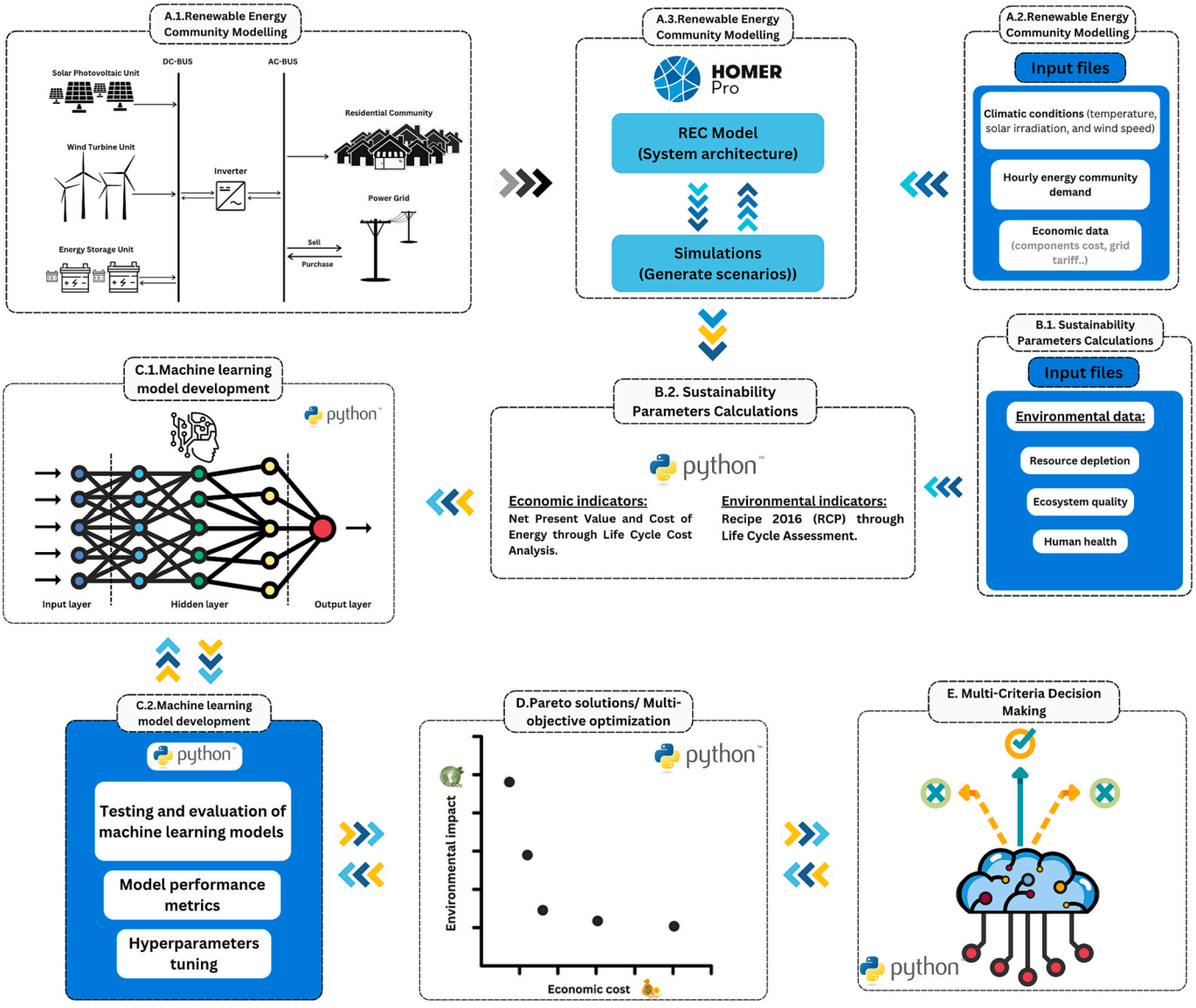

Fig. 1. Framework for the renewable energy community system design optimization.

$$P_{PV} = Y_{PV} f_{PV} \left(\frac{G_T}{G_{T,STC}}\right)\left[1 + \alpha_P\left(T_C - T_{C,STC}\right)\right] \quad (1)$$

Where Y_{PV} stands for the PV output under typical operating conditions (kW), G_T and $G_{T,STC}$ represents incident solar radiation in the current time step (kW/m^2), at the standard temperature condition (kW/m^2), respectively. f_{PV} is the PV array's derating factor (%), α_P refers to the temperature coefficient of power measured in (%/°C), T_C represents for the PV's temperature in °C, and $T_{C,STC}$ stands for the PV array's temperature at the standard temperature conditions (i.e., 25 °C). the T_C is calculated using the following equation:

$$T_C = \left(\frac{T_a + \left(T_{C,NOCT} - T_{a,NOCT}\right)\left(\frac{G_T}{G_{T,NOCT}}\right)}{1 + \left(T_{C,NOCT} - T_{a,NOCT}\right)\left(\frac{G_T}{G_{T,NOCT}}\right)}\right) \cdot \left(\frac{1 - \left(\eta_{mp,STC}\right)\left(\frac{1-\alpha_P T_{C,STC}}{\tau_\alpha}\right)}{\frac{\alpha_P \eta_{mp,STC}}{\tau_\alpha}}\right) \quad (2)$$

where α is the solar absorption, τ is the solar transmittance of the PV array, η_c is the electrical conversion efficiency of the PV array, $\eta_{mp,STC}$ is the maximum power point efficiency under standard test conditions, expressed in (%),α_P is the temperature coefficient of power (%/°C), Tc and Ta are the cell and ambient temperature, $T_{c,STC}$ and $T_{C,NOCT}$ are the cell temperature under; standard test conditions (25 °C); and nominal operating cell temperature, respectively.

b. Wind turbine

In Homer, the wind turbine is modeled as a device that converts wind kinetic energy into DC or AC electricity. The wind electricity production is calculated using a three-stage approach; First, HOMER calculates the wind speed at the wind turbine's hub height. The amount of electricity the wind turbine produces at the given wind speed and constant air density is then calculated. Finally, HOMER adjusts the power output figure as needed to reflect the actual air density. HOMER employs the following equation to calculate the wind speed at the hub height:

$$U_{hub} = U_{anem} \cdot \frac{ln\left(\frac{z_{hub}}{z_0}\right)}{ln\left(\frac{z_{anem}}{z_0}\right)} \quad (3)$$

Where U_{hub}, U_{anem}, z_{hub}, and $z_0$are the wind speed at the hub of the wind turbine, and the wind speed at anemometer height (m/s), the wind

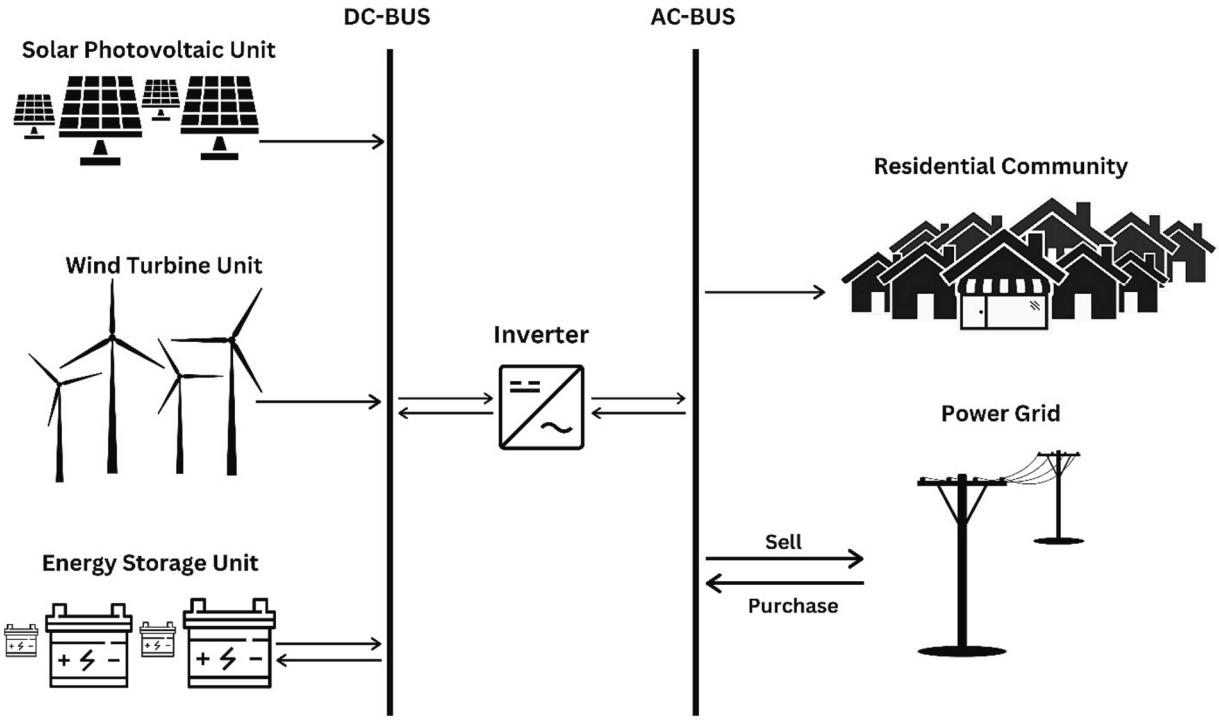

Fig. 2. Schematic of the proposed renewable energy community system.

velocity at the wind turbine hub height, the anemometer height above the surface roughness length, and the anemometer height, respectively. The wind turbine power generation can be calculated using the equation below:

$$P_{WTG} = \left(\frac{\rho}{\rho_0}\right).P_{WTG,STC} \tag{4}$$

Where P_{WTG}, $P_{WTG,STC}$ are the power generation of wind turbine, and the wind turbine output at the standard condition (kW), ρ and ρ_0 are the actual air density, and the air density at standard condition, respectively.

c. Battery and charge controller

The mathematical model used by HOMER defines a single battery as a device with the capacity to store a certain amount of direct current (DC) power with a fixed energy efficiency. In order to provide power regulation to and from the battery, the system needs a charge controller. It monitors if the battery is completely charged or needs to be recharged. By performing this, the battery is protected from damage. The system's battery capacity can be determined using following equation Eq. (5):

$$N_{bat} = \frac{E_d.n_d}{V_{bat}.Ah.DOD} \tag{5}$$

Where n_d, E_d, $V_{bat}, Ah, and\ DOD$ are the days of autonomy, the daily energy demand, the battery voltage score, the ampere hours, and the battery system depth of discharge, respectively.

2.2. Economic assessment

In this work, the economic evaluation of 2000 energy system scenarios is carried out using the LCC approach. The LCC technique's core idea is the use of a future-cost approach. This involves employing a discounting method to determine the present value of all costs spent over the system's lifespan. The levelized cost of energy (LCOE) and net present cost (NPC) are the two primary economic measures used in the LCC approach.

The NPC of a system is the present value of all costs minus the present value of all income generated throughout the system's lifespan. Capital expenses, replacement costs, operations and maintenance costs, and the purchased electricity from the grid are all included in the costs. Salvage value and grid sales revenue are among the revenues, mathematically expressed as stated in Eq. (6):

$$C_{NPC} = \frac{C_{ann,tot}}{CRF\left(i, R_{proj}\right)} \tag{6}$$

Where $C_{ann,tot}, CRF, i, R_{proj}$, are the annualized cost ($/year), the capital recovery factor, the real interest rate (%), and the project lifetime (year), respectively. The Capital Recovery Factor (CRF) is calculated using the following formula:

$$CRF(i,N) = \frac{i(1+i)^N}{(1+i)^N - 1} \tag{7}$$

Where N, and i are the number of years, and the real interest rate (%), respectively.

The LCOE is commonly used as a benchmark to compare the cost of different power generation technologies, the LCOE calculates the system's average cost per kWh of electrical energy and is computed utilizing Eq. (8):

$$LCOE = \frac{C_{ann,tot}}{E_{prim,AC} + E_{prim,DC} + E_{grid,sales}} \tag{8}$$

Where $C_{ann,tot}$ is the annualized cost ($/year), $E_{prim,AC}$ is the AC primary load served (kWh/year), $E_{prim,DC}$ is the DC primary load served (kWh/year), $E_{grid,sales}$ is the total grid sales (kWh/year).

2.3. Environmental assessment

Along with the LCC approach for evaluating the configurations of the renewable energy community systems' economic performance, the environmental impact of each configuration is evaluated from an using the life cycle assessment (LCA). By examining the product lifecycle from a global viewpoint, this technique offers a comprehensive assessment of

the local impacts on the environment. LCA evaluates the product under the "cradle-to-grave" approach [44] while considering several environmental factors. Goal and scope definition, inventory analysis, impact assessment, and interpretation are the four key steps that follow a specific sequence to set the LCA methodology, the LCA approach was standardized under the ISO14040 series [45–47]. The following subsections comprehensively explain these stages:

2.3.1. Goal and scope definition

The system, its boundaries, and the functional unit are the three primary scopes included in this phase. The system boundary would be established using the "cradle-to-gate" concept, with the end user distribution networks excluded. The functional unit in this study is the capacity of renewable energy community system (i.e., photovoltaic system, wind turbine, battery capacity installed), and the quantity of energy amount purchased from the grid.

2.3.2. Inventory analysis

The second stage of the LCA procedure, inventory analysis, quantifies the input and output materials and the energy consumed throughout the installation and operation of the renewable energy community. In the current study, takes into account a number of impact sources, including the operation of the plant over the course of the entire time horizon (LCI_i^{OP}), transportation of materials and finished equipment units to the site (LCI_i^{TR}),and utility energy consumption and the manufacturing of equipment by the system over the course of its lifetime (LCI_i^{MP}). The inventory entries can be stated mathematically in Eq. (9):

$$LCI_i^{TOT} = LCI_i^{MP} + LCI_i^{TR} + LCI_i^{OP} \tag{9}$$

Where LCI_i^{TOT}, LCI_i^{MP}, LCI_i^{TR}, *and* LCI_i^{OP} represent the total life cycle inventory, the manufacturing processes, the transportation tasks, and the plant operation associated with the elementary flow i, respectively.

2.3.3. Impact assessment

In this step, the ReCiPe method involves converting Inventory data into endpoint scores, which are then classified into three categories: human health, ecological systems, and resource depletion [48]. These categories are combined to create a normalized indicator metric (RCP) for each residential renewable energy community system configuration. The impact values related to each effect category can be stated mathematically in Eq. (10):

$$IMP_e = \sum_i \Theta_{ei}.LCI_i^{TOT} \tag{10}$$

where Θ_{ei} represents for the characterization factor that connects endpoint impact category e with elementary flow i.

The endpoint impact categories e are then combined into damage categories (DAMd), which are then normalized and combined into a single final indication RCP for each residential renewable energy community system configuration. Mathematically, the RCP score can be expressed as shown in Eqs. (11 to 12):

$$DAM_d = \sum_{e \epsilon ID_d} IMP_e \forall d \tag{21}$$

$$RCP = \sum_d \delta_d \varepsilon_d DAM_d \forall d \tag{32}$$

The provided equation includes DAM_d, which is the endpoint score for damage category d. To normalize endpoint data for different damage categories, the $\delta_d$is a factor is based on the use of land and extraction of materials in the European setting. While ε_d is the weight factor based on values recommended in the ReCiPe 2016 framework.

2.3.4. Interpretation

An analysis of the findings is provided at this stage. In this context, the LCC approach, which employs NPC for estimating the future cost and levelized cost of energy as first objective function, and the environmental impact indicator RCP as second objective function to evaluate each renewable energy community system configuration using a multiobjective function optimization algorithm. As a result, Pareto set optimum solutions can be obtained. They provide more insight about various renewable energy community system configurations and, consequently, encourage decision-makers to choose the options that best suit their needs/preferences.

2.4. Data generation and preparation

For machine learning algorithms to be effective, training data generation is essential for decision tree algorithms. The quantity and quality of the training data have a direct impact on the generalization and accuracy of the model. The local optimal algorithm may converge to a suboptimal solution without sufficient and representative training data. Therefore, it is essential to carefully design and generate the training dataset for local optimization algorithms to ensure they can effectively identify the proper optimal solution [49].

First, we developed a renewable energy community system using Homer Pro software, considering the specific energy demands of the community. We then identified all feasible and possible combinations of scenarios. To design each configuration, we focused on changing the size of different components such as the PV system, wind turbine, battery energy system, dispatch strategy, and the amount of energy purchased and sold to the grid. This allowed us to explore different combinations of renewable energy systems and generate all the possible ways to meet community energy demands. After collecting data from the HOMER Pro software, we obtained an extensive dataset of 2000 renewable energy community system scenarios that are feasible to cover the community's energy demand.

2.5. Optimization procedure

2.5.1. Training of the machine learning model

The training of a Random Forest Regression model using a dataset of 2000 scenarios for community-based renewable energy systems generated from the HOMER Pro software is the first step in the optimization process. This dataset includes several renewable energy system configurations together with the associated economic metrics (e.g. levelized cost of energy and net present cost) and environmental impact indicators (e.g. ReCiPe scores). Notably, Python was used to execute the LCA and LCC calculations, providing the essential economic and environmental indicators for the machine learning model's training.

The Random Forest Regression algorithm is used for establishing a functional relationship between the system configurations used as input parameters and the economic metrics and environmental impact indicators utilized as output variables. Each tree in the Random Forest is constructed using a different subset of the training data and a random subset of features. The final prediction is then made by aggregating the predictions of all the individual trees in the forest. The dataset is provided to the model during training to assist it in identifying correlations and patterns between system parameters and related metrics. The model develops the capacity to predict the economic and environmental performance of various system configurations as a result of this training process. The inherent trade-offs between the cost of energy and environmental impact could be captured by the machine learning model, which leads to the enhancement of decision-making and design optimization.

2.5.2. Performance evaluation

Following the training phase, the trained Random Forest Regression model's performance is evaluated using the right metrics. A validation dataset distinct from the training dataset is used to do this. The model's capacity for predicting economic metrics and environmental impact

indicators is assessed using metrics like Mean Absolute Error (MAE), Explained Variance Score (EVS), and R-squared (R2). These performance indicators offer insightful information about the model's accuracy and generalizability, given in Eqs. (13 to 15):

$$MAE = \frac{1}{n}\sum_{i=1}^{n}|y_i - y_i^{'}| \tag{43}$$

$$R^2 = 1 - \frac{\sum_{i=1}^{n}(y_i - y_i^{'})^2}{\sum_{i=1}^{n}(y_i - y_i^{\hat{}})^2} \tag{54}$$

$$EVS = 1 - \frac{Var(y - y^{'})}{Var(y)} \tag{65}$$

Where $y_i, y_i^{'}$, *and* $y_i^{\hat{}}$, are the actual value, the predicted value, and the mean of the predicted value, respectively, and Var represents the variance.

2.5.3. Prediction of objective function values

After the Random Forest Regression model has been successfully trained and assessed, it is used to predict the values of the objective functions, especially the levelized cost of energy (LCOE) and the environmental effect (RCP), for a certain system configuration. The trained model produces predictions of the LCOE and RCP values when the desired system configuration is introduced into it. Despite the need for costly simulations or computations, this predictive capacity allows the examination of various system designs.

2.5.4. Identification of optimal design

In order to provide insight into decision-making, we varied the weights for each objective function, specifically the levelized cost of energy (LCOE) and environmental impact (RCP). Moreover, a multi-criteria decision-making approach based on Weighted Sum Model (WSM) is proposed to help the stakeholders to see beyond the LCC and LCA based on selection criteria to choose the most appropriate scenario optimal solution for the desired energy community and interpret the effect of various economic parameters on the sustainable performance of REC. Using this method, we can determine the optimum designs for achieving a balance between reducing energy costs and decreasing the impact on the environment. We can identify the configurations that offer the best balance between cost and environmental sustainability using methods such Pareto optimization, which considers the predicted values of LCOE and RCP for various system configurations. The outcome is identifying one or more optimum designs which satisfy the intended objectives.

Our objective is to design a REC, through the development of a framework that integrates life cycle assessment and life cycle cost analysis approaches through a machine learning model.

3. Case study

The proposed renewable energy community model will be applied to a residential community in Tarragona, Spain, that consists of a neighborhood of 100 buildings as depicted in Fig. 3. The major inputs for the energy community system modeling in HOMER Pro are electrical load, solar irradiation, air temperature, components cost, and energy prices.

3.1. Electricity consumption data

A python programming in-house tool was used the gather the real hourly electricity consumption per household in kWh within the residential sector of Spain on an hourly basis from the Datadis platform [50]. The daily and seasonal demand profiles are depicted on Fig. 4. The daily average power consumption is 691.34 kWh with a peak of 70.35 kW.

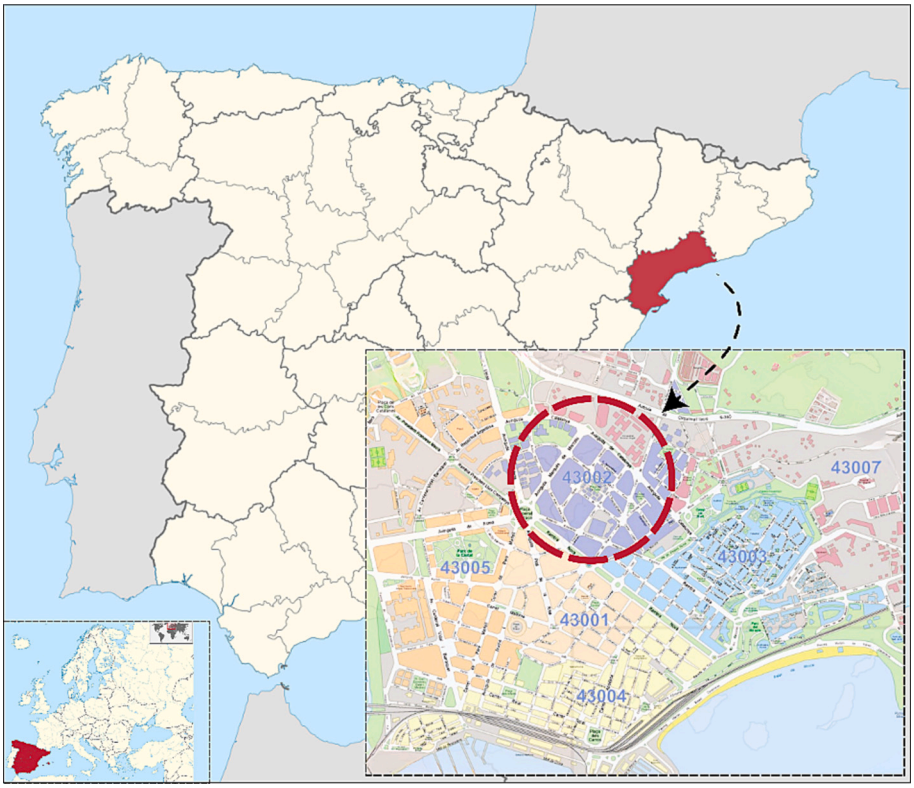

Fig. 3. 3 Location of the simulated renewable energy community in the city of Tarragona, Spain.

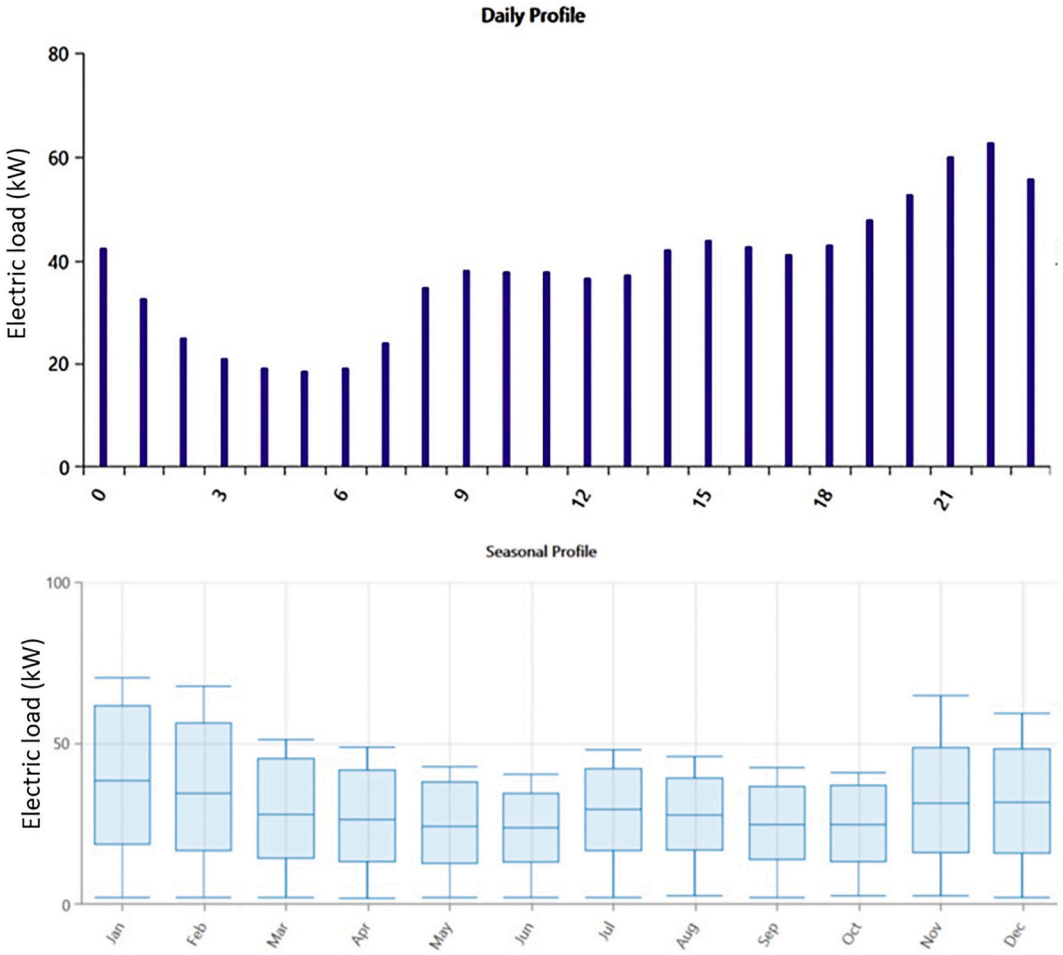

Fig. 4. Daily profile (the upper figure) and the seasonal profile (the below figure) for electricity demand of an energy community for 100 residential buildings in Tarragona, Spain.

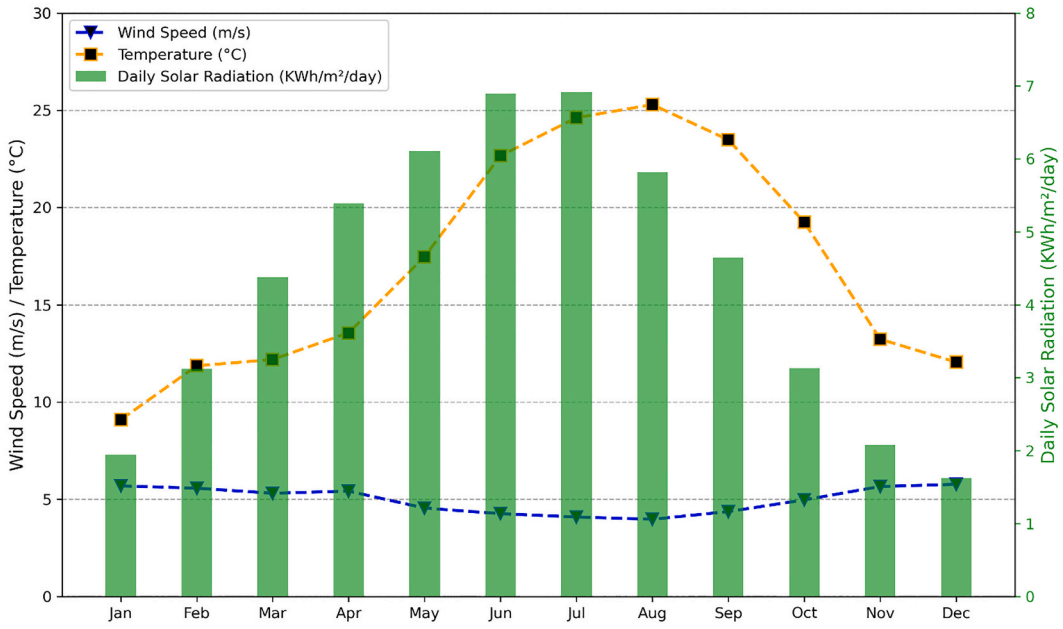

Fig. 5. Climatic condition of the renewable energy community location in Tarragona, Spain.

3.2. Climate profile

We have collected the climatic data specifically for our renewable energy community case study in Tarragona. These data were obtained from a weather station located in Tarragona and the gathered data were processed and prepared for utilization in Homer Pro. The dataset comprises of wind speed, ambient temperature, and sun radiation. The average monthly values for various climate variables are shown in Fig. 5.

3.3. Economic and environmental data

The project parameters such as the discount rate, inflation rate, annual capacity shortage and the project lifetime as well as the economic data including the capital cost, operation and maintenance cost and replacement cost for all the requirements of the renewable energy community can be found in Table 1.

The LCA data are extracted from the Ecoinvent database [51], these data include the impact of various REC units and grid utility based on ReCiPe 2016 methodology are given in Table 2.

4. Results and discussions

The results of the current study are presented in three main areas. First, the developed data-driven model is comprehensively analyzed through key indicators such as R-squared score, mean absolute error, and explained variance. The study's second section analyzes the effectiveness of REC sizes in an optimization framework using a developed Machine Learning model taking into account the environmental and economic parameters. The goal is to improve the feasibility of the REC by optimizing the design parameters of the photovoltaic system, wind turbine, and battery electrical energy system. Finally, by including multi-objective optimization/Pareto solutions and using multi-criteria decision-making approaches in order to assist the decision-making process, the study successfully shows the optimal design of the REC. This comprehensive approach ensures an in-depth evaluation and promotes well-informed REC decision-making.

4.1. Data driven performance metrics

We have examined the performance of our LCOE and RCP models, using a variety of measures to assess their accuracy and reliability. The performance indicators R-squared score, mean absolute error, and explained variance for the LCOE and RCP models are presented in Table 3.

As shown in the table, a significant R-squared score of 0.9498 was attained by the LCOE model, which indicates a strong linear relationship between the predicted and actual values of the levelized cost of energy; this indicates that the model can account for approximately 94.98% of the uncertainty in the LCOE.

Furthermore, the low mean absolute error (MAE) of 0.004 demonstrates the precision of the LCOE model prediction. Similarly, the RCP model showed an excellent R-squared score of 0.99968, indicating an almost perfect fit of the predicted values to the actual RCP data. According to the strong R-squared value, the model can explain almost 99.97% of the RCP variance. It is important to note that the mean absolute error (MAE) of 398.08(representing 0.03%) provides insights into the average magnitude of the errors made by the model. Fig. 6. illustrates the comparison of the actual and predicted values of LCOE on the left side and RCP on the right side; the color bar employing absolute error integrated into the figures represents the prediction accuracy, with darker blue indicating a higher level of accuracy.

Table 1
The project and economic data of renewable energy community systems parameters.

		Value	Ref.
Project parameters	Discount rate (%)	7	[52]
	Inflation rate (%)	5.89	[52]
	Annual capacity shortage (%)	0	[53]
	Project lifetime (years)	25	[53]
Grid parameters	Grid Power Price ($/kWh)	0.298	[54]
	Grid sellback Price ($/kWh)	0.06	[54]
PV system parameters ($/kW)	Capital cost ($)	1073	[55]
	Replacement cost ($)	1073	[55]
	O&M cost ($)	10	[55]
	Lifetime (years)	25	[55]
Converter parameters ($/kW)	Capital cost ($)	300	[55]
	Replacement cost ($)	300	[55]
	O&M cost ($)	0	[55]
	Lifetime (years)	15	[55]
Wind turbine ($/kW)	Capital cost ($)	2100	[53]
	Replacement cost ($)	2100	[53]
	O&M cost ($)	36	[53]
	Lifetime (years)	25	[53]
Storage parameters ($/kWh)	Capital cost ($)	189	[56]
	Replacement cost ($)	189	[56]
	O&M cost ($)	1.36	[56]
	Lifetime (years)	5	[56]
	Nominal-voltage (Volts)	12	[56]
	Round Trip Efficiency (%)	85	[56]

4.2. Optimization results

In Fig. 7, a parallel coordinate plot illustrates the relationships between design parameters, including photovoltaic system (PV), wind turbine (WT), and battery electrical energy storage (BEES) capacities and target variables as ReCiPe 2016 aggregated impact factor (RCP) and levelized cost of energy (LCOE) for various energy mix scenarios. The lines linking the axes reflect several energy mix possibilities, and each axis represents a different variable value. Fig. 7a shows how the lines are colored using a gradient color scale (Viridis) depending on the LCOE values (Fig. 7b shows the RCP as the target variable), visually depicting the range and magnitude of LCOE within the dataset. The LCOE values corresponding to the selected colors are displayed in the figure's color bar on the right side. The parallel coordinate provides insightful information as well as support for decision-makers in selecting the optimal energy mix scenario. Decision-makers can easily evaluate the links between parameters and variables across several scenarios by visually comparing the energy mix scenarios based on the design parameters and target variables. As illustrated in Fig. 7a, the figure identifies the design parameters associated with the lowest LCOE, enabling the determination of the most cost-effective energy mix combination. Similarly, Fig. 7b depicts the design parameters associated with the lowest impact on the environment (RCP).

In Fig. 7, a parallel coordinate plot showcases insightful findings regarding the sizing patterns of various objective functions, specifically cost optimization and environmental optimization, in various energy mix scenarios. The plot reveals that scenarios with the lowest LCOE prioritize larger allocations of PV capacity, signaling its cost-effectiveness. Conversely, scenarios focused on minimizing environmental impact feature a more equitable distribution of PV and WT capacities, highlighting the importance of renewable energy source diversification for environmental sustainability. Furthermore, Fig. 7 provides insights into the impact of changing design parameters on other variables, supporting informed decision-making based on priorities and requirements.

Fig. 8 represents the Multi-Objective Optimization for Optimal Scenario Selection by Pareto Sets Analysis. It comprises two sub-figures, Fig. 8a and Fig. 8b. In Fig. 6a, the focus is on the Pareto sets analysis. It showcases the trade-off objectives: Levelized Cost of Energy (LCOE) and its environmental impact in terms of RCP for all solutions and the equal weights of the two objective functions (balanced weight = 0.5), which presents a significant reduction of the environmental impact with a relatively low cost increase. The base case represents the current situation, in which all the energy comes from the grid. On the other hand,

Table 2
The environmental impact of the renewable energy community system based on ReCiPe 2016.

	Functional unit	Damage category (Pt)			
Unit		Ecosystem quality	Human health	Resource depletion	Specific ReCiPe 2016 impact factor (final score) (Pt)
Photovoltaic system	kW	47.53333	126.01000	123.75000	297.29333
Wind turbine	kW	8.70550	15.24500	63.82000	87.77125
Battery energy storage system	kg	0.07520	0.27666	0.66785	1.01970
Electricity	kWh	0.01166	0.0025494	0.014206	0.035961

Table 3
Performance Metrics for LCOE and RCP Models.

Metric	LCOE	RCP
R-squared Score	0.9498	0.99968
Mean Absolute Error	0.0040	398.08
Explained Variance	0.9490	0.99968

Fig. 8b complements Fig. 8a by offering insights into decision-making. The Pareto optimum solutions are represented clearly for various weights.

The results of multi-objective optimization provide valuable insight into the trade-offs between levelized energy cost and environmental impact. By examining different options, we can observe considerable differences in the Levelized Cost of Energy (LCOE) and the Environmental Impact (RCP). The results indicate a significant increase in LCOE of roughly 396.64% when comparing the minimum cost solution to the minimum environmental impact solution. In addition to this increase, there has been a significant reduction in the environmental impact of around 61.65%. Moreover, there is a significant difference in the LCOE of around 44.66% between the minimal cost solution and the balanced solution, while the environmental impact increases by almost 55.75%. Compared to the base case scenario, the minimum environmental impact solution shows a drop in LCOE of approximately 25.95%, demonstrating improved cost-efficiency while emphasizing environmental sustainability. Additionally, a 9.89% rise in environmental impact above the basic scenario indicates a reduced environmental impact. We also observe a notable drop in LCOE of roughly 85.04% when comparing the base case solution to the minimum cost solution. Conversely, the environmental impact has increased by around 18.71%. Similarly, the balanced solution shows a notable increase in cost-effectiveness, with a significant drop in LCOE of about 72.86% compared to the base scenario. There is a trade-off between cost and environmental sustainability. Nevertheless, the Environmental Impact increased by about 27.02% compared to the basic scenario. These comparisons reveal the effectiveness of the multi-objective optimization in achieving trade-offs and improvements compared to the base-case scenario. Fig. 9 complements Fig. 8b, by providing insightful information about the capacities of PV (Photovoltaic), WT (Wind Turbine), and BEES (Battery Electrical Energy Storage) for each weight. As well as comparing the capacity installed of each technology and emphasizing the influence of weights on these values.

As shown in Fig. 9, the min impact solution (weight = 0), the focus is to get the optimal energy mix scenario that minimizes the impact on the environment; in this energy mix scenario, we have a relatively balanced capacity allocation among the PV, WT, and BEES reflects a strategy that aims to reduce the overall environmental footprint. The capacity installed for each technology is given as follows: PV (115.3 kW), WT (231 kW), and BEES (192 units); this is a moderately balanced approach towards utilizing multiple renewable energy sources while considering the environmental consequences. Moving to the balanced solution (weight = 0.5), in this solution, the aim is to get the optimal energy mix scenario by balancing the economic benefits and the environmental impact; this energy mix scenario, compared to min impact solution, showcases an increase in the PV and WT capacities by approximately 69.30%(195 kW), 112.55% (310 kW), respectively. However, the BEES capacity decreases from the min impact solution (192 units) to the balanced solution (25 units) by 86.98%. Lastly, the main objective of the min cost solution (weight = 1) is to get the most cost-effective energy mix by minimizing the LCOE. In this scenario, the PV capacity has a

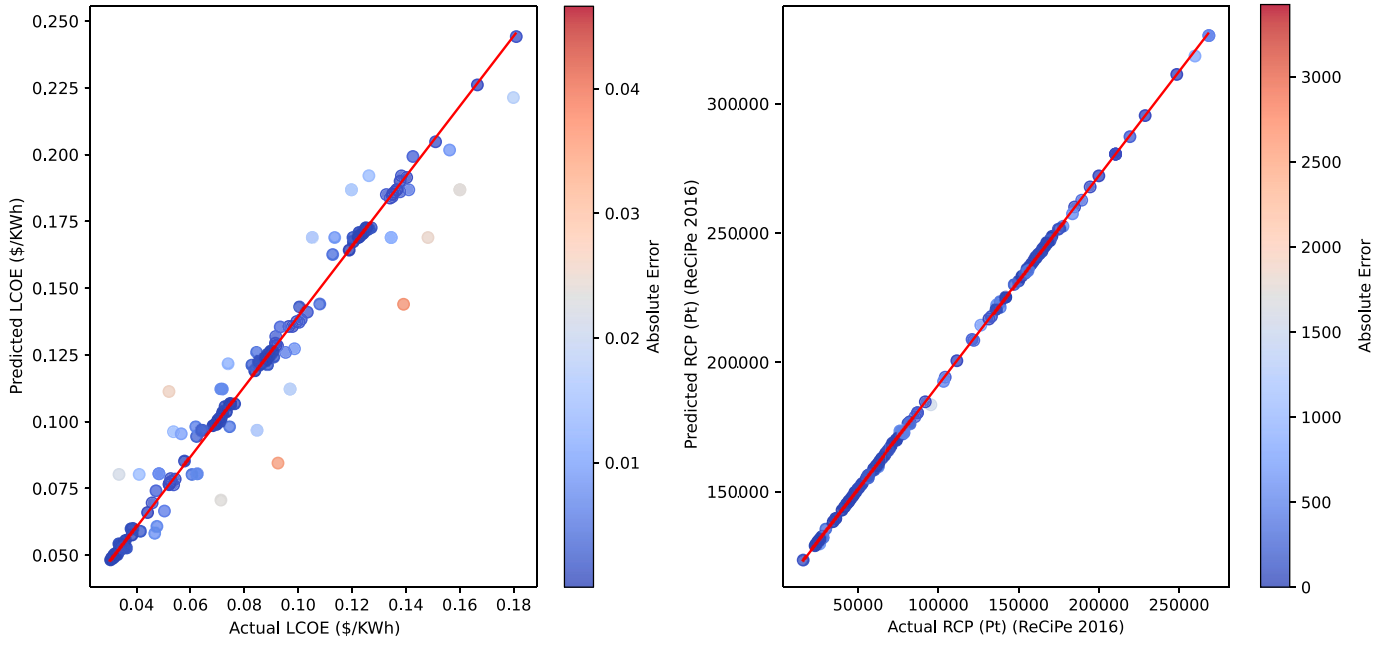

Fig. 6. Comparison of actual and predicted LCOE (left figure) and RCP (right figure).

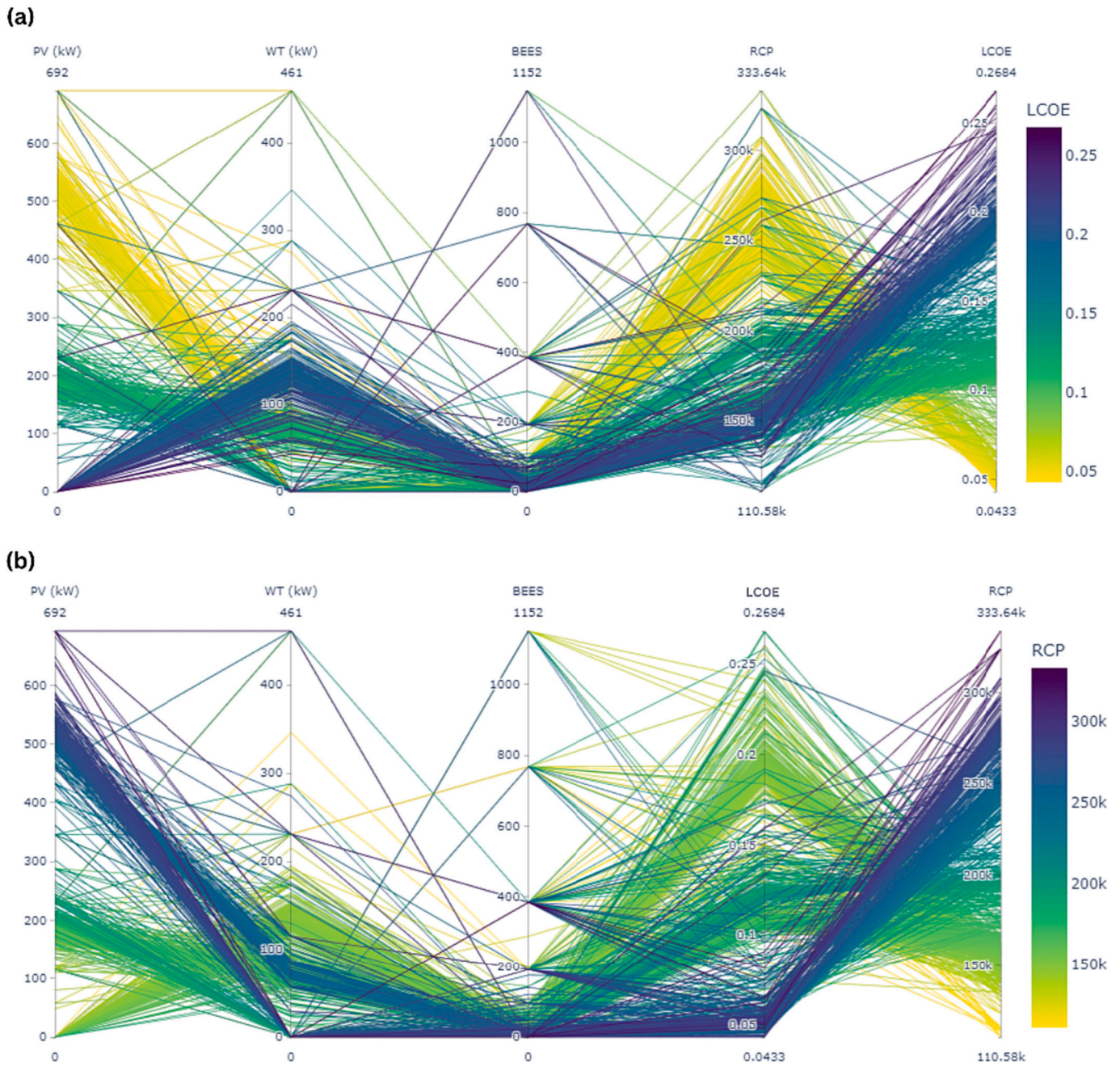

Fig. 7. Parallel coordinate plot: design parameters and targets analysis for LCOE (a) and RCP(b) optimization.

higher capacity of 555 kW; this represents an increase of 184.62% and 381.56% compared to the balanced and min impact solutions, respectively. The min-cost solution has a lower WT capacity of 87 kW. This decrease represents 82.45% and − 62.81% compared to the balanced and min impact solutions, respectively. These comparisons emphasize the variation in capacity installed through different solutions; the minimum cost solution highlights cost effectiveness, leading to a higher PV capacity while a lower WT capacity and no energy storage. The Balanced solution strives for a balanced approach with a large WT capacity and modest PV and energy storage capacities. The minimum impact approach prioritizes reducing the impact on the environment, leading to a balanced capacity distribution across all technologies.

Fig. 10 displays a pie chart for the "Min impact" solution, which highlights the distribution of impacts across three categories: resource depletion, human health, and ecosystem quality. The largest segment of impact is resource depletion at 54.1%, followed by human health at 32.3%, and the smallest category is ecosystem quality at 13.6%. In addition, the corresponding bar chart below shows that the PV system, wind turbine, and BEES system have varying levels of impact on these three categories. Notably, the grid has the least visible impact.

Fig. 11 displays the "Min cost" solution, which presents a pie chart that exhibits a distinct distribution: human health and resource depletion each make up 42%, while ecosystem quality accounts for 16.1%. The accompanying bar chart reflects these priorities, displaying different impacts for the PV system, wind turbine, BEES system, and grid, with the focus on cost minimization. On the other hand, the "Min impact" solution appears to prioritize reducing resource depletion more than the "Min cost" solution, which takes a more balanced approach between resource depletion and human health impacts. Moreover, the "Min cost" solution seems to assign slightly more importance to ecosystem quality than the "Min impact" solution.

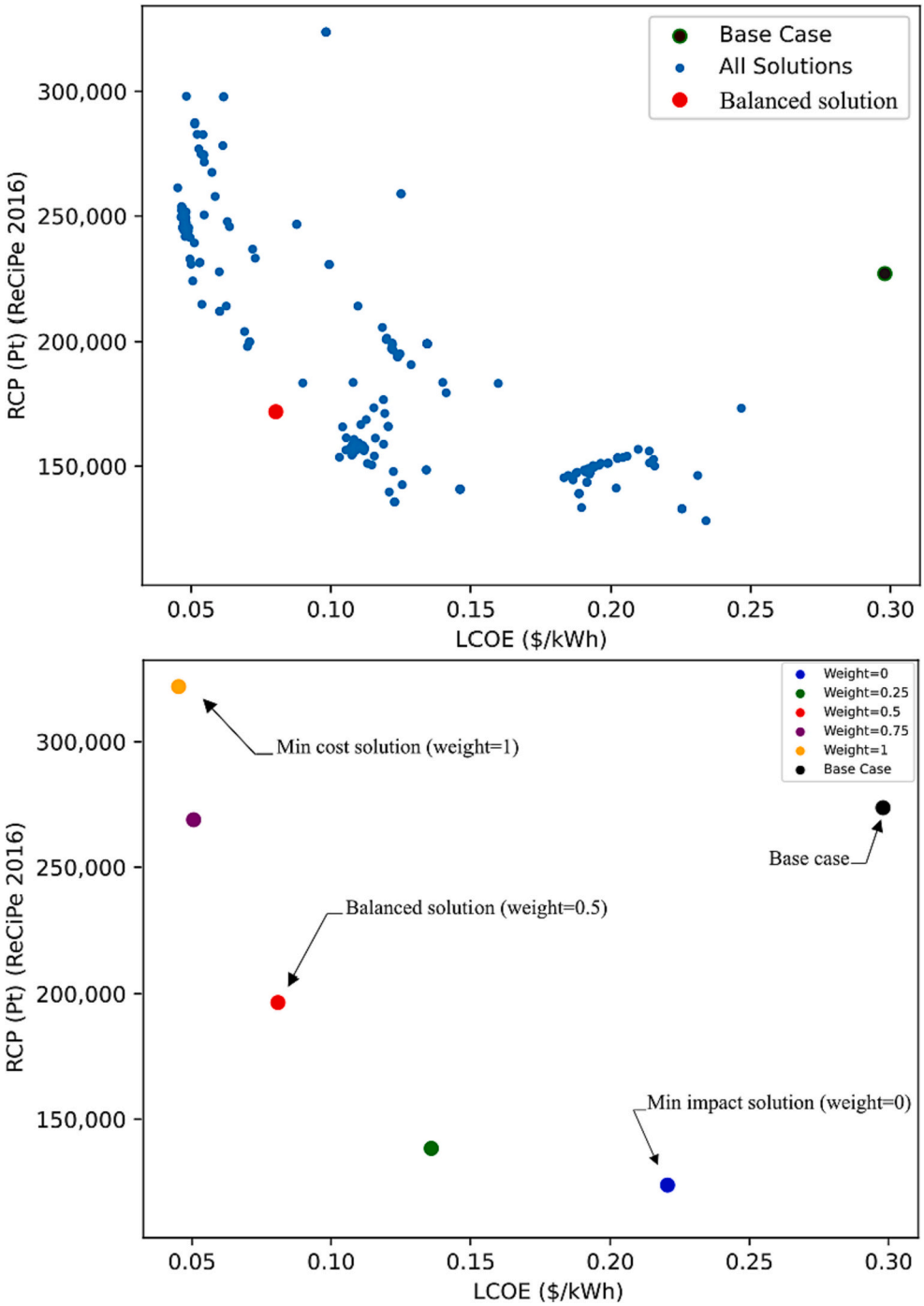

Fig. 8. Multi-Objective Optimization for Optimal Scenario Selection: Pareto Sets Analysis.

4.3. Comparison of the proposed optimization and NSGA-II

This section compares the proposed optimization optimal solution against Non-dominated Sorting Genetic Algorithm II (NSGA-II), in the comparative analysis of multi-objective optimization results, the Pareto front generated by our optimization algorithm (illustrated in blue in Fig. 12) exhibits a broader coverage across the objective space than the NSGA-II Pareto front (depicted in red), indicating a more extensive exploration of the solution space, particularly with respect to the environmental impact metric, RCP. While the NSGA-II Pareto front appears to converge upon a more narrowly defined region, suggesting a potentially more focused search for economically efficient solutions, our Pareto front presents a diversity of trade-offs, affording decision-makers a wider spectrum of options to balance economic and environmental objectives. Notably, there are regions where our Pareto front achieves lower RCP values at comparable levels of LCOE, and vice versa, underscoring areas where one approach outperforms the other. To quantitatively substantiate these observations, further analysis is warranted, utilizing metrics such as hypervolume to assess the coverage and convergence properties, and diversity metrics to evaluate the distribution of solutions. Additionally, sensitivity analysis could elucidate the robustness of these solutions, while statistical testing across multiple optimization runs might confirm the significance of the observed differences. The preliminary visual assessment suggests that our optimization approach can generate a set of diverse solutions, which is instrumental for decision-makers needing to navigate complex trade-off

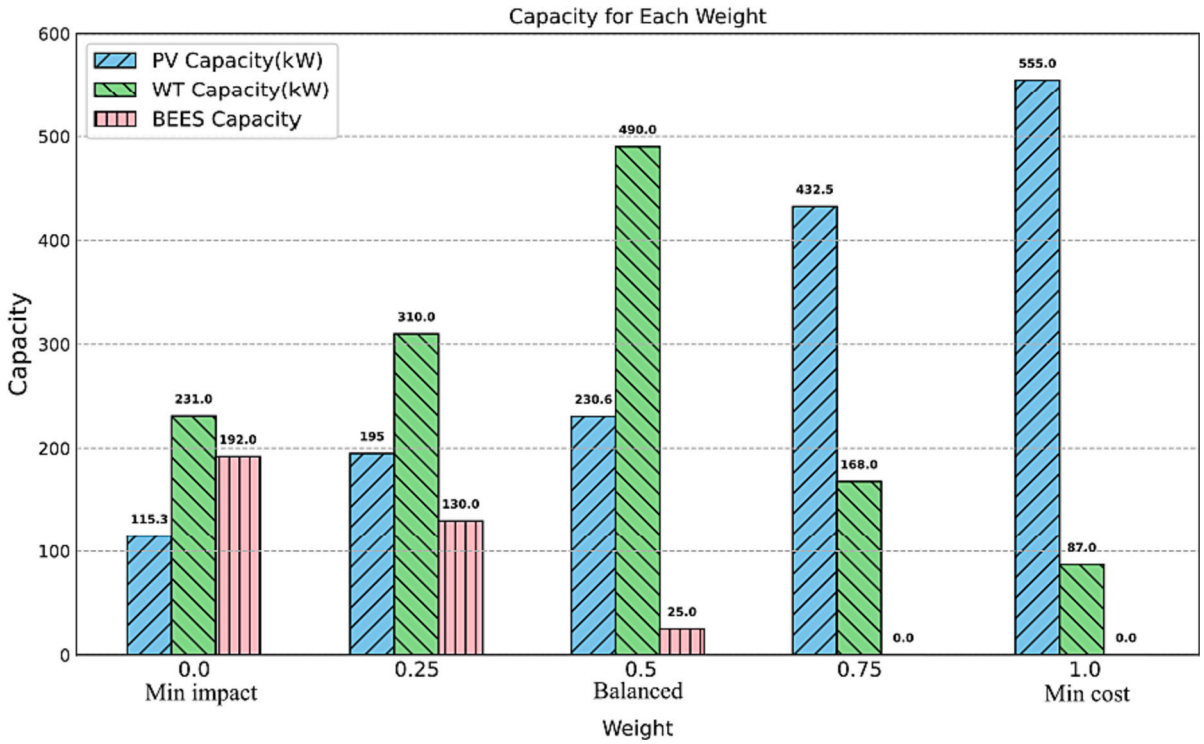

Fig. 9. Comparative analysis of capacity for different energy sources at varying weights.

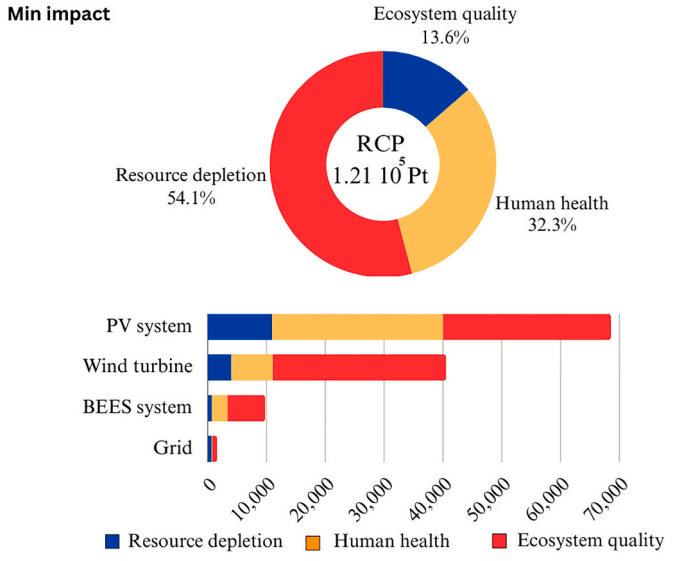

Fig. 10. Graphical features of the environmental impact assessment of the min impact solution.

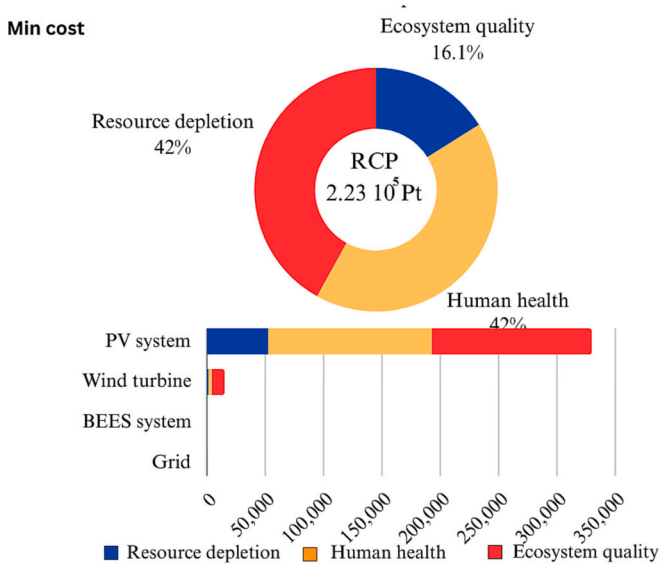

Fig. 11. Graphical features of the environmental impact assessment of the min cost solution.

scenarios.

In conclusion, the results of each energy mix scenario rely on their unique objectives and preferences. If cost-effectiveness is the main priority, PV is the preferred choice due to its lower LCOE, although it may have a more significant environmental impact than WT. On the other hand, when minimizing environmental impact is the primary objective, WT is the better option as it has a lower environmental footprint. In contrast, BEES tend to have a moderate allocation in different situations. These situations illustrate the trade-offs and relationships between cost, environmental sustainability, and the characteristics of each technology when designing renewable energy systems.

The results presented in this study are based on our specific case study data, which includes the geographical location, resource availability, local environmental and economic data, and energy demand. It is important to note that if the same methodology framework is used for a different case study, the results may vary significantly.

5. Conclusion

In this research paper, we developed a data-driven framework to design the renewable energy community (REC) considering its techno-economic failures and environmental impact. In order to assist the stakeholders' decision-making, the study tends to optimize the size of the

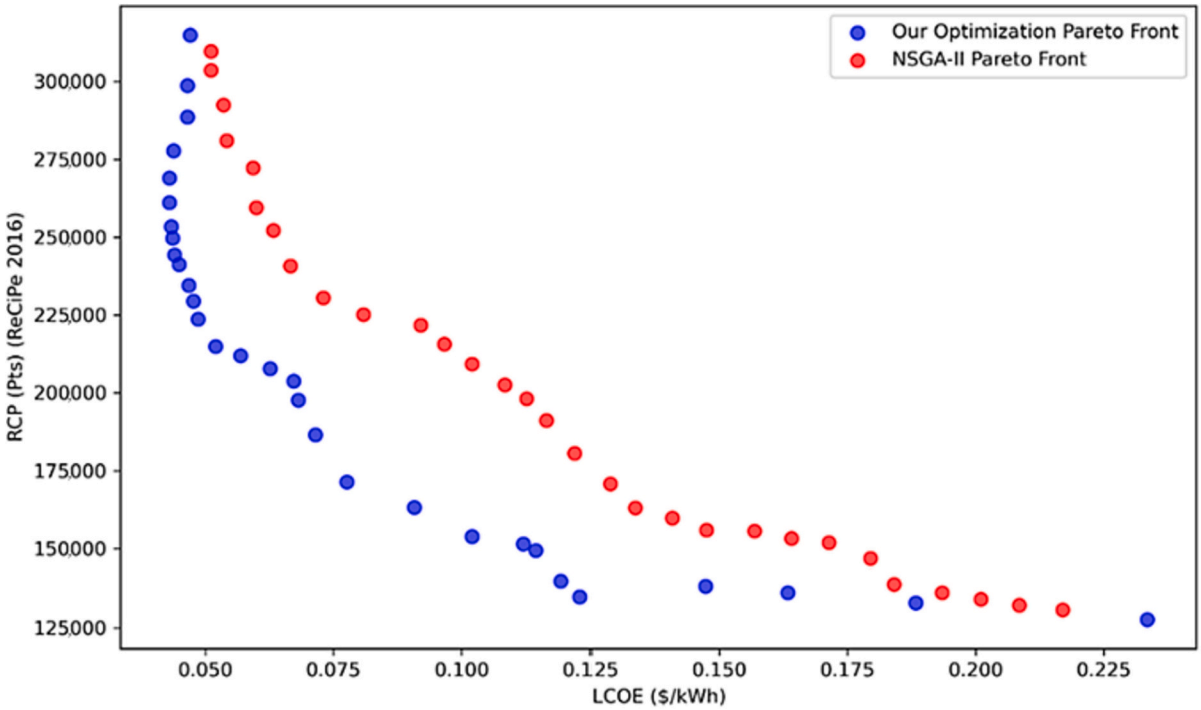

Fig. 12. Comparison of Multi-objective optimization results.

REC source of energy technologies used such as: photovoltaic systems, wind turbines, and battery electrical energy systems under energy, economic, and environmental criteria.

In this context, Homer Pro and an in-house tool developed in Python programming language that incorporates a machine learning algorithm, life cycle cost (LCC), life cycle assessment (LCA) calculations of REC model. Furthermore, a multi-objective optimization model is established to minimize the LCC and LCA parameters with consideration for maximizing green energy use.

A multi-criteria decision-making approach based on Weighted Sum Model (WSM) is proposed to help the stakeholders to see beyond the LCC and LCA based on selection criteria to choose the most appropriate scenario optimal solution for the desired energy community and interpret the effect of various economic parameters on the sustainable performance of REC. The summary of the findings for our case study is the following:

- Compared to the existing base case (LCOE = 0.297 $/kWh, RCP =2.734 10^5 Pts) (all demand is covered from the grid), the minimum environmental impact solution (LCOE = 0.220 $/kWh, RCP =1.242 10^5 Pts) shows a drop in LCOE by 25.95%, demonstrating improved cost-efficiency while emphasizing environmental sustainability.
- The balanced solution (LCOE = 0.080 $/kWh, RCP =1.965 10^5 Pts) shows a notable increase in cost-effectiveness, with a significant drop in LCOE by 72.86% compared to the base scenario. Nevertheless, the Environmental Impact increased by about 27.02% compared to the basic scenario.
- The LCOE in the minimum cost-optimal solution (LCOE = 0.044 $/kWh, RCP =2.237 10^5 Pts) is approximately 85.04% lower than the base case, while the environmental impact of the minimum cost solution is about 18.32% higher than the base case.
- The results revealed a significant increase in LCOE by 3.96 times when comparing the minimum cost solution to the minimum environmental impact solution. Additionally, there was a significant 61.65% reduction in environmental impact.
- The data-driven framework suggests that PV installed capacity has the biggest impact on the cost-effectiveness of the REC model, while the low PV, WT, and BEES capacity is suggested for the min environmental impact.
- The developed methodology has also provided a guideline for the REC system sizing with the optimal size range of REC system components.

Overall, this study provides an effective tool for the techno-economic and environmental assessment of the REC in the residential sector, which can be applied to plan its integration into the existing energy community.

CRediT authorship contribution statement

Youssef Elomari: Writing – original draft, Visualization, Software, Methodology, Investigation, Formal analysis, Data curation, Conceptualization. **Carles Mateu:** Writing – review & editing, Supervision. **M. Marín-Genescà:** Writing – review & editing, Supervision, Investigation. **Dieter Boer:** Writing – review & editing, Supervision, Resources, Project administration, Funding acquisition, Conceptualization.

Declaration of competing interest

The authors declare that they have no known competing financial interests or personal relationships that could have appeared to influence the work reported in this paper.

Data availability

Data will be made available on request.

Acknowledgements

The authors would like to acknowledge financial support from the "Ministerio de Ciencia, Innovación y Universidades" of Spain (PID2021-127713OA-I00, PID2021-123511OB-C31, PID2021-123511OB-C33, PID2021-124139NB-C22 funded by MCIN/AEI/10.13039/501100011033/FEDER, UE & TED2021-129851B-I00 funded by MCIN/

AEI/10.13039/501100011033 and by the "European Union NextGenerationEU/PRTR).

References

[1] International Energy Agency. Energy efficiency: Buildings. The global exchange for energy efficiency policies, data and analysis. https://www.iea.org/topics/buildings (accessed Jun. 01, 2023).

[2] Canale L, Di Fazio AR, Russo M, Frattolillo A, Dell'Isola M. An overview on functional integration of hybrid renewable energy systems in multi-energy buildings. Energies Feb. 01, 2021;14(4). https://doi.org/10.3390/en14041078. MDPI AG.

[3] European Commission. LEVEL(S) - Taking action on the TOTAL impact of the construction sector. Accessed: Jun. 01, 2023. [Online]. Available, http://ec.europa.eu/environment/eussd/buildings.htm.

[4] Motuziene V, Rogoža A, Lapinskiene V, Vilutiene T. Construction solutions for energy efficient single-family house based on its life cycle multi-criteria analysis: a case study. J Clean Prod Jan. 2016;112:532–41. https://doi.org/10.1016/J.JCLEPRO.2015.08.103.

[5] United Nations. Open working group proposal for sustainable development goals, sutainable dev. https://sustainabledevelopment.un.org/focussdgs.html (accessed Jun. 01, 2023).

[6] European Commission. REPowerEU: Joint European Action for more affordable, secure, and sustainable energy. Press release 2022. https://commission.europa.eu/strategy-and-policy/priorities-2019-2024/european-green-deal/repowereu-affordable-secure-and-sustainable-energy-europe_en (accessed Jun. 01, 2023).

[7] European Comission. EU solar energy strategy. Press release 2022. https://energy.ec.europa.eu/topics/renewable-energy/solar-energy_en.

[8] European Comission. Energy communities. https://energy.ec.europa.eu/topics/markets-and-consumers/energy-communities_en (accessed Jun. 01, 2023).

[9] European Comission. RENewAble Integration and SuStainAbility iN energy CommunitiEs | RENAISSANCE Project | Fact Sheet | H2020 | CORDIS | European Commission. https://cordis.europa.eu/project/id/824342 (accessed Jun. 01, 2023).

[10] Karunathilake H, Hewage K, Mérida W, Sadiq R. Renewable energy selection for net-zero energy communities: life cycle based decision making under uncertainty. Renew Energy Jan. 2019;130:558–73. https://doi.org/10.1016/J.RENENE.2018.06.086.

[11] Karunathilake H, Perera P, Ruparathna R, Hewage K, Sadiq R. Renewable energy integration into community energy systems: a case study of new urban residential development. J Clean Prod Feb. 2018;173:292–307. https://doi.org/10.1016/j.jclepro.2016.10.067.

[12] Kolokotsa D. The role of smart grids in the building sector. Energ Buildings Mar. 15, 2016;116:703–8. https://doi.org/10.1016/j.enbuild.2015.12.033. Elsevier Ltd.

[13] Javadi MS, Gough M, Nezhad AE, Santos SF, Shafie-khah M, Catalão JPS. Pool trading model within a local energy community considering flexible loads, photovoltaic generation and energy storage systems. Sustain Cities Soc Apr. 2022;79. https://doi.org/10.1016/j.scs.2022.103747.

[14] Parra D, Norman SA, Walker GS, Gillott M. Optimum community energy storage for renewable energy and demand load management. Appl Energy 2017;200:358–69. https://doi.org/10.1016/j.apenergy.2017.05.048.

[15] J M, Zhu YL Jianmin. Optimal energy management in community micro-grids. 2023.

[16] Rao BV, Stefan M, Schwalbe R, Karl R, Kupzog F, Kozek M. Stratified control applied to a three-phase unbalanced low voltage distribution grid in a local peer-to-peer energy community. Energies (Basel) Jun. 2021;14(11). https://doi.org/10.3390/en14113290.

[17] Gribiss H, Aghelinejad MM, Yalaoui F. Configuration selection for renewable energy community using MCDM methods. Energies (Basel) Mar. 2023;16(6):2632. https://doi.org/10.3390/en16062632.

[18] Felice A, Rakocevic L, Peeters L, Messagie M, Coosemans T, Ramirez Camargo L. Renewable energy communities: do they have a business case in Flanders? Appl Energy Sep. 2022;322. https://doi.org/10.1016/j.apenergy.2022.119419.

[19] Houben N, et al. Optimal dispatch of a multi-energy system microgrid under uncertainty: a renewable energy community in Austria. Appl Energy May 2023;337. https://doi.org/10.1016/j.apenergy.2023.120913.

[20] Tang Y, Zhang Q, Mclellan B, Li H. Study on the impacts of sharing business models on economic performance of distributed PV-battery systems. Energy Oct. 2018;161:544–58. https://doi.org/10.1016/j.energy.2018.07.096.

[21] Cui S, Wang YW, Shi Y, Xiao JW. An efficient peer-to-peer energy-sharing framework for numerous community prosumers. IEEE Trans Industr Inform Dec. 2020;16(12):7402–12. https://doi.org/10.1109/TII.2019.2960802.

[22] Cui S, Wang Y-W, Li C, Xiao J-W. Prosumer community: a risk aversion energy sharing model. IEEE Trans Sustain Energy 2020;11(2):828–38.

[23] Brummer V. Community energy – benefits and barriers: A comparative literature review of Community Energy in the UK, Germany and the USA, the benefits it provides for society and the barriers it faces. Renew Sustain Energy Rev Oct. 01, 2018;94:187–96. https://doi.org/10.1016/j.rser.2018.06.013. Elsevier Ltd.

[24] Orehounig K, Evins R, Dorer V. Integration of decentralized energy systems in neighbourhoods using the energy hub approach. Appl Energy Sep. 2015;154:277–89. https://doi.org/10.1016/j.apenergy.2015.04.114.

[25] Luo L, et al. Optimal siting and sizing of distributed generation in distribution systems with PV solar farm utilized as STATCOM (PV-STATCOM). Appl Energy Jan. 2018;210:1092–100. https://doi.org/10.1016/j.apenergy.2017.08.165.

[26] Han ME, Alston M, Gillott M. A multi-vector community energy system integrating a heating network, electricity grid and PV production to manage an electrified community. Energ Buildings Jul. 2022;266. https://doi.org/10.1016/j.enbuild.2022.112105.

[27] Piazza G, Delfino F, Bergero S, Di Somma M, Graditi G, Bracco S. Economic and environmental optimal design of a multi-vector energy hub feeding a local energy community. Appl Energy Oct. 2023;347. https://doi.org/10.1016/j.apenergy.2023.121259.

[28] Bahramara S, Moghaddam MP, Haghifam MR. Optimal planning of hybrid renewable energy systems using HOMER: a review. Renew Sustain Energy Rev 2016;62:609–20. https://doi.org/10.1016/j.rser.2016.05.039. Elsevier Ltd.

[29] Cardoso G, et al. Optimal investment and scheduling of distributed energy resources with uncertainty in electric vehicle driving schedules. Energy Jan. 2014;64:17–30. https://doi.org/10.1016/j.energy.2013.10.092.

[30] Cutler D, et al. REopt: A platform for energy system integration and optimization [Online]. Available: www.nrel.gov/publications; 2017.

[31] Tozzi P, Jo JH. A comparative analysis of renewable energy simulation tools: performance simulation model vs. system optimization. Renew Sustain Energy Rev 2017;80:390–8. https://doi.org/10.1016/j.rser.2017.05.153. Elsevier Ltd.

[32] Behzadi MS, Niasati M. Comparative performance analysis of a hybrid PV/FC/battery stand-alone system using different power management strategies and sizing approaches. Int J Hydrogen Energy Jan. 2015;40(1):538–48. https://doi.org/10.1016/j.ijhydene.2014.10.097.

[33] Raji Atia NYMI. Optimization of a PV-wind-diesel system using a hybrid genetic algorithm. 2012.

[34] Yang H, Lu L, Zhou W. A novel optimization sizing model for hybrid solar-wind power generation system. Solar Energy Jan. 2007;81(1):76–84. https://doi.org/10.1016/j.solener.2006.06.010.

[35] Akinyele D. Analysis of photovoltaic mini-grid systems for remote locations: a techno-economic approach. Int J Energy Res Mar. 2018;42(3):1363–80. https://doi.org/10.1002/er.3886.

[36] Nasser A, Reji P. Optimal planning approach for a cost effective and reliable microgrid. 2016.

[37] I RAGM, Bansal RKMI Ajay Kumar. Optimization of hybrid PV/wind energy system using meta particle swarm optimization (MPSO). 2023.

[38] Elomari Y, Norouzi M, Marín-Genescà M, Fernández A, Boer D. Integration of solar photovoltaic systems into power networks: a scientific evolution analysis. Sustainability (Switzerland) Aug. 01, 2022;14(15). https://doi.org/10.3390/su14159249. MDPI.

[39] Gaviria JF, Narváez G, Guillen C, Giraldo LF, Bressan M. Machine learning in photovoltaic systems: a review. Renew Energy Aug. 01, 2022;196:298–318. https://doi.org/10.1016/j.renene.2022.06.105. Elsevier Ltd.

[40] Ferrara M, et al. Design optimization of renewable energy systems for NZEBs based on deep residual learning. Renew Energy Oct. 2021;176:590–605. https://doi.org/10.1016/j.renene.2021.05.044.

[41] Ahmed W, et al. Machine learning based energy management model for smart grid and renewable energy districts. IEEE Access 2020;8:185059–78. https://doi.org/10.1109/ACCESS.2020.3029943.

[42] Ananda Kumar S, et al. A novel islanding detection technique for a resilient photovoltaic-based distributed power generation system using a tunable-Q wavelet transform and an artificial neural network. Energies (Basel) Aug. 2020;13(6). https://doi.org/10.3390/en13164238.

[43] Khatib T, Elmenreich W. An improved method for sizing standalone photovoltaic systems using generalized regression neural network. Int J Photoenergy 2014;2014. https://doi.org/10.1155/2014/748142.

[44] Nemerow NL, Agardy FJ, Sullivan Patrick, Salvato JA. Environmental engineering. Water, wastewater, soil, and groundwater treatment and remediation. Wiley; 2009.

[45] ISO 14044 Environmental management-Life cycle assessment-Requirements and guidelines Management environnemental-Analyse du cycle de vie-Exigences et lignes directrices. 2006.

[46] ISO 14044 Environmental management-Life cycle assessment-Requirements and guidelines Management environnemental-Analyse du cycle de vie-Exigences et lignes directrices. 2008.

[47] Environmental management-Life cycle assessment-Principles and framework Management environnemental-Analyse du cycle de vie-Principes et cadre [Online]. Available, www.iso.org; 2006.

[48] Huijbregts MAJ, et al. ReCiPe2016: a harmonised life cycle impact assessment method at midpoint and endpoint level. Int J Life Cycle Assess Feb. 2017;22(2):138–47. https://doi.org/10.1007/s11367-016-1246-y.

[49] Wagner M, Day J, Neumann F. A fast and effective local search algorithm for optimizing the placement of wind turbines. Renew Energy Mar. 2013;51:64–70. https://doi.org/10.1016/j.renene.2012.09.008.

[50] DATADIS. La plataforma de datos de consumo eléctrico, "Asociación de Empresas Eléctricas (ASEME).". https://datadis.es/ (accessed Mar. 04, 2023).

[51] Ecoinvent 3.8 dataset documentation. 2023.

[52] Comisión Nacional de los Mercados y la Competencia, "Documento de consulta pública sobre la propuesta de metodología de cálculo de la tasa de retribución financiera de la actividad de producción de energía eléctrica a partir de fuentes de energía renovables, cogeneración y residuos para el siguiente periodo regulatorio 2020–2025 Expediente: INF/DE/113/18 1. Antecedentes y fundamentos jurídicos." [Online]. Available, www.cnmc.es.

[53] Al-Badi A, Al Wahaibi A, Ahshan R, Malik A. Techno-economic feasibility of a solar-wind-fuel cell energy system in Duqm, Oman. Energies (Basel) Aug. 2022;15(15). https://doi.org/10.3390/en15155379.

[54] Análisis | ESIOS electricidad · datos · transparencia. https://www.esios.ree.es/es/analisis/1739?vis=1&start_date=23-02-2023T00%3A00&end_date=23-02-202

3T23%3A55&compare_start_date=22-02-2023T00%3A00&groupby=hour&compare_indicators=1001 (accessed Mar. 20, 2023).
[55] I. Renewable Energy Agency. Renewable power generation costs in 2021 - Executive summary. 2023.
[56] Carroquino J, Escriche-Martínez C, Valiño L, Dufo-López R. Comparison of economic performance of lead-acid and li-ion batteries in standalone photovoltaic energy systems. Appl Sci (Switzerland) Apr. 2021;11(8). https://doi.org/10.3390/app11083587.